AJNR

Decreased Diffusivity in the Caudate Nucleus of Presymptomatic Huntington Disease Gene Carriers: Which Explanation?

M.L. Mandelli, M. Savoiardo, L. Minati, C. Mariotti, D. Aquino, A. Erbetta, S. Genitrini, S. Di Donato, M.G. Bruzzone and M. Grisoli

AJNR Am J Neuroradiol 2010, 31 (4) 706-710
doi: https://doi.org/10.3174/ajnr.A1891
http://www.ajnr.org/content/31/4/706

ORIGINAL RESEARCH

M.L. Mandelli
M. Savoiardo
L. Minati
C. Mariotti
D. Aquino
A. Erbetta
S. Genitrini
S. Di Donato
M.G. Bruzzone
M. Grisoli

Decreased Diffusivity in the Caudate Nucleus of Presymptomatic Huntington Disease Gene Carriers: Which Explanation?

BACKGROUND AND PURPOSE: The neostriatum is known to be affected in HD. In this work, our aim was to determine whether microstructural and volumetric alterations occur in the neostriatum of presymptomatic HD gene carriers and in patients with early-stage HD.

MATERIALS AND METHODS: We studied a group of 15 presymptomatic gene carriers who were far from the estimated symptom onset (16% probability of developing the disease within 5 years), a group of 9 patients with early symptomatic HD, and 2 groups of age-matched controls. Volumetric MR imaging and DWIs were acquired, and statistical analyses were performed on the volumes of the caudate nucleus and putamen and on the corresponding MD measurements.

RESULTS: Neostriatal volumes were significantly smaller in both presymptomatic HD gene carriers and symptomatic patients with respect to controls. However, whereas the diffusivity in the caudate nucleus was increased in the symptomatic patients, it was decreased in the presymptomatic gene carriers.

CONCLUSIONS: Altered diffusivity and reduced volume of the caudate nucleus in presymptomatic HD gene carriers indicate that the neostriatum is affected well before the onset of symptoms. The observed initial decrease and subsequent increase of MD might be related to the combined effect of increased oligodendroglial population, putatively a developmental abnormality, and incipient neurodegeneration.

ABBREVIATIONS: CAG = cytosine-adenine-guanine; DWI = diffusion-weighted imaging; FMRIB = Functional Magnetic Resonance Imaging of the Brain; HD = Huntington disease; MD = mean diffusivity; n.s. = not significant; MPRAGE = magnetization-prepared rapid acquisition of gradient echo; ROI = region of interest; TFC = total functional capacity; TIV = total intracranial volume; UHDRS = Unified Huntington Disease Rating Scale

HD is a neurodegenerative disorder caused by an abnormal expansion of CAG repeats coding for polyglutamine in a gene termed *IT15*, located on chromosome 4p16.3.[1] The disease is characterized by increasingly severe motor impairment, cognitive decline, and behavioral changes leading to functional disability. Symptoms commonly appear between 35 and 50 years of age but may appear at any time. Death occurs, on average, 15–20 years after the onset of symptoms.

The main pathologic feature of HD is loss of neurons in the striatum,[1] accompanied by fibrillary astrocytosis and diffuse brain atrophy of variable severity. A few studies have evaluated the potential usefulness of the volume of the striatum as a neurobiologic marker of disease progression, demonstrating that it may be used to predict the clinical onset of symptoms and to evaluate the efficacy of potential novel treatments.[2-5]

DWI is an MR imaging technique that allows in vivo investigation of the microstructural properties of tissues by using the random motion of water molecules as a probe. Measurement of the directionally averaged diffusivity can provide information on tissue integrity at the microstructural level, because degeneration usually results in increased diffusivity.[6] Several studies have demonstrated increased diffusivity in the striatum in symptomatic HD,[7-9] and 1 study also found a correlation with disease severity.[8]

Even though volumetric changes in the caudate nucleus and putamen of presymptomatic HD gene carriers have been consistently reported, comparatively few results are available regarding diffusional changes; in particular, only 1 study has shown increased diffusivity in the putamen,[9] and alterations in the caudate nucleus were not found. Here, we report results from a cross-sectional study on the volumetric and diffusional changes in the neostriatum of presymptomatic and symptomatic patients with HD, conducted by using manually drawn planar regions of interest and segmented volumes to measure the MD in the caudate nucleus and putamen.

Received June 16, 2009; accepted after revision August 19.

From the Neuroradiology Department (M.L.M., M.S., L.M., D.A., A.E., M.G.B., M.G.), Eighth Neurology Department (C.M., S.G., S.D.D.), and Science Direction Unit (L.M.), Fondazione Istituto Nazionale Neurologico "Carlo Besta," Milan, Italy; Bioengineering Department (M.L.M.), Politecnico di Milano, Milan, Italy; and Psychiatry Department (L.M.), Brighton and Sussex Medical School, Brighton, UK.

Please address correspondence to Maria Luisa Mandelli, MD, Dipartimento di Neuroradiologia, Istituto Nazionale Neurologico "Carlo Besta," Via Celoria, 11, I-20133 Milan, Italy; e-mail: mandelli@istituto-besta.it

DOI 10.3174/ajnr.A1891

Materials and Methods

Subjects

Fifteen presymptomatic HD gene carriers and 9 patients with symptomatic HD were studied; control subjects were also recruited in 2 groups matching the average age of the HD groups (Table 1). All participants gave written informed consent for the study, which was conducted in accordance with the Declaration of Helsinki and institutional guidelines.

Control subjects had no history of neurologic, psychiatric, or other medical disturbances and had normal findings on brain MR

Table 1: Demographic and clinical data[a]

	Pre-HD Controls	Pre-HD Subjects	HD Controls	HD Patients (Stage I)
Number of subjects	14	15	11	9
Age (yr)	31 ± 6.7	32 ± 6.6	49.7 ± 13.5	46.7 ± 8.5
Sex (M:F)	5:9	7:8	5:6	7:2
CAG repeats, expanded allele	–	42.6 ± 3.1	–	45.1 ± 2.8
TFC score	–	13	–	11.8 ± 1.4
Disease duration (yr)	–	–	–	3.9 ± 3.6
UHDRS score	–	–	–	17.3 ± 3.9

[a] Values are expressed as mean ± SD.

imaging. All presymptomatic and symptomatic patients with HD scored positive on a molecular test, with >38 CAG repeats in the *huntingtin* gene (Table 1). As confirmed by a Mann-Whitney *U* test, there was no significant difference in the number of CAG triplet repeats between the 2 groups.

Presymptomatic HD gene carriers, aware of their genetic status, were recruited among individuals requesting genetic testing for the HD mutation, which was performed according to the International Huntington's Association and World Federation of Neurology guidelines.[10] None of them had any clinical signs or symptoms of the disease or any abnormal findings on brain MR imaging; according to the model proposed by Langbehn et al,[11] the probability of developing clinical symptoms in the following 5 years was estimated to be 16 ± 23%.

As confirmed by clinical assessment of the motor symptoms by using the UHDRS,[12] the patients with symptomatic HD had manifest symptoms of the disease. All were in stage I according to the specifications of Marder et al.[13] The capacity in functional tasks, determined with the TFC scale,[13] and the disease duration (ie, the number of years since the appearance of motor symptoms) are given in Table 1.

MR Imaging

Subjects were scanned on a 1.5T Avanto MR imaging system (Siemens, Erlangen, Germany). Although choreic movements were observed in all symptomatic patients and were particularly disabling in 2, they did not interfere with the MR imaging studies. Structural imaging, performed for positioning and to exclude other pathologies, included axial proton attenuation/T2-weighted images (TR = 3500 ms, TE = 17/84 ms, section thickness = 6 mm), coronal turbo spin-echo T2-weighted images (TR = 4500 ms, TE = 143 ms, section thickness = 4 mm), and axial gradient-echo $T2^*$-weighted images (TR = 833 ms, TE = 26 ms, flip angle = 20°, section thickness = 5 mm). 3D T1-weighted images were acquired by means of the MPRAGE sequence (TR = 1640 ms, TE = 2 ms, 1-mm^3 isotropic voxel, 160 sagittal sections). DWI was performed by means of a twice-refocused single-shot spin-echo echo-planar sequence (TR = 7500 ms, TE = 80 ms, matrix = 192 × 256, FOV = 180 × 240 mm, section thickness = 2.5 mm, no intersection gap) with diffusion-sensitizing gradients along 12 directions by using b-values of 0 and 1000 s/mm^2. The acquisitions were repeated 5 times to improve the signal intensity–to-noise ratio.

Morphometric Study of the Neostriatum

The volumes of the caudate nucleus and putamen were measured on the T1-weighted MPRAGE images. An initial segmentation and labeling were performed automatically by means of the Individual Brain Atlases Statistical Parametric Mapping toolbox, developed in Matlab (MathWorks, Natick, Massachusetts).[14,15] The resulting segmentations of the 2 structures were subsequently refined, section-by-section on the 3 planes, by an experienced operator. The posterior limit of the segmented caudate nucleus corresponded to the posterior margin of the body at the level of the posterior third segment of the cella media of the lateral ventricle.[16] The tail of the caudate nucleus was not included due to its difficult identification. An example of the segmentation is shown in Fig 1.

For the purpose of statistical analysis, the volumes of the caudate nucleus and putamen were normalized to the total intracranial volume of each subject.

Diffusional Study of the Neostriatum

DWIs were corrected for eddy current distortion by means of the software provided with the scanner and were subsequently corrected for head motion by using the FMRIB Linear Image Registration Tool software (FMRIB, University of Oxford, Oxford, United Kingdom) with 12 df. MD maps were then calculated by means of the DTIStudio software (Johns Hopkins University, Baltimore, Maryland) by averaging the eigenvalues of the diffusion tensor, estimated by using a multivariate linear regression model.[17]

Circle planar regions of interest of a fixed 5-mm diameter for measurement of the MD were drawn on the T1-weighted images twice for each subject by 2 neuroradiologists in 2 separate sessions and then were coregistered with the T2-weighted echo-planar images. ImageJ software (National Institute of Mental Health, Bethesda, Maryland) was used. The intraclass correlation coefficient was calculated to assess the agreement between the 2 raters, and the intrarater reliability was estimated on 10 scans evaluated by the first rater.

In addition, to further confirm the results obtained with manually drawn regions of interest, we measured the average diffusivity by using the segmented caudate nucleus and putamen volumes obtained from morphometric analysis. In contrast with planar regions of interest, this method does not imply the choice of a section by the operator. To obtain the average diffusivity values for each structure, we performed the following steps for each participant: 1) DWI volumes were coregistered with the T1 image by using Statistical Parametric Mapping 5 (Wellcome Trust Centre for Neuroimaging, London, United Kingdom); 2) each segmentation mask of the caudate nucleus and putamen (1 inside, 0 outside the structure) was transferred from the T1 image space to the DWI image space by applying the coregistration matrix; 3) to ensure exclusion of CSF-containing voxels, we removed all voxels with MDs $>1.6 \times 10^{-3}$ mm^2 s^{-1} from the mask, which was also eroded by 2 voxels to reduce potential partial volume effects; and 4) the average value of voxels included in the mask was calculated.

Statistical Analysis

Statistical analysis was performed by using the Statistical Package for the Social Sciences, Version 16.0 software (SPSS, Chicago, Illinois). To avoid potential confounding effects due to the age difference between the presymptomatic gene carriers and the symptomatic patients, we performed comparisons separately by using distinct age-matched control groups. After confirming that the data were normally distributed by means of Shapiro-Wilk normality tests, we performed 2-tailed *t* tests on the volume and MD measurements. We checked for outliers by considering 2.5 SDs from the mean as a cutoff. To further confirm our findings, we also performed nonparametric Mann-Whitney *U* tests. For both tests, the significance threshold was set at $P < .05$.

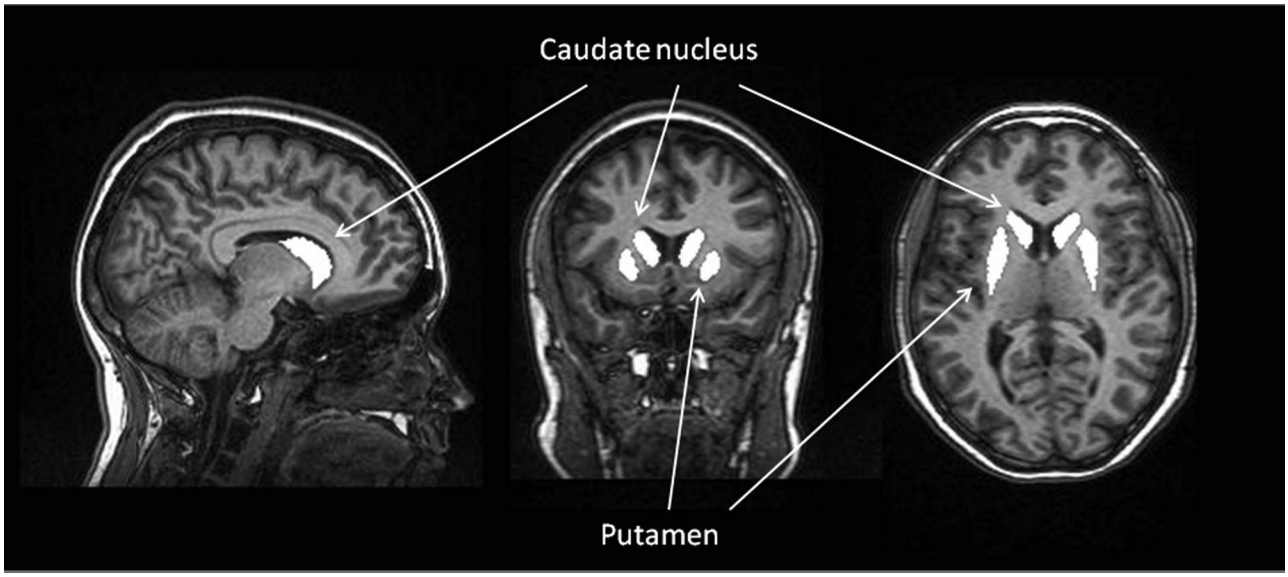

Fig 1. The caudate nucleus and putamen extracted from the T1-weighted MR images (sagittal, coronal, and axial views).

Table 2: Results from volume measurements[a]

	Controls for HD Gene Carriers (n = 14)	HD Gene Carriers (n = 15)	P Value	Controls for HD Patients (n = 11)	HD Patients (n = 9)	P Value
Caudate/TIV	0.545 ± 0.099	0.452 ± 0.052	.004	0.494 ± 0.076	0.264 ± 0.074	<.001
	0.559 (0.346–0.744)	0.451 (0.348–0.556)	.01	0.472 (0.342–0.645)	0.251 (0.115–0.412)	<.001
Putamen/TIV	0.548 ± 0.058	0.464 ± 0.073	.002	0.477 ± 0.076	0.248 ± 0.089	<.001
	0.535 (0.432–0.664)	0.468 (0.317–0.611)	.002	0.484 (0.324–0.630)	0.234 (0.069–0.427)	<.001

[a] Values are expressed as SD (upper row) and median (range, lower row); significance values are for the t test (upper row) and Mann-Whitney U test (lower row).

Table 3: Results from diffusivity ($\times 10^{-3}$ mm^2 s^{-1}) measurements[a]

Structure	Method	Controls for HD Gene Carriers (n = 14)	HD Gene Carriers (n = 15)	P Value	Controls for HD Patients (n = 11)	HD Patients (n = 9)	P Value
Caudate	Planar ROI	0.717 ± 0.02	0.697 ± 0.03	.04	0.716 ± 0.02	0.806 ± 0.04	<.001
		0.714 (0.677–0.758)	0.696 (0.637–0.757)	.03	0.711 (0.668–0.763)	0.811 (0.729–0.883)	<.001
Putamen	Planar ROI	0.711 ± 0.02	0.714 ± 0.03	n.s.	0.701 ± 0.02	0.801 ± 0.06	.002
		0.723 (0.665–0.758)	0.720 (0.663–0.768)	n.s.	0.700 (0.661–0.741)	0.801 (0.679–0.923)	.003
Caudate	Volume average	0.743 ± 0.02	0.721 ± 0.02	.005	0.735 ± 0.02	0.788 ± 0.04	.001
		0.748 (0.701–0.785)	0.723 (0.683–0.758)	.006	0.742 (0.697–0.773)	0.792 (0.708–0.869)	.009
Putamen	Volume average	0.735 ± 0.02	0.733 ± 0.02	n.s.	0.725 ± 0.02	0.809 ± 0.04	<.001
		0.737 (0.692–0.778)	0.735 (0.692–0.774)	n.s.	0.716 (0.689–0.762)	0.820 (0.727–0.893)	<.001

[a] Values are expressed as mean ± SD (upper row) and median (range, lower row); significance values are for the t test (upper row) and Mann-Whitney U test (lower row).

Results

Morphometric Study

Values were normally distributed, and there were no outliers. As reported in Table 2, the volumes of the caudate nucleus and putamen were reduced in patients with HD with respect to controls ($P < .001$). They were also reduced in presymptomatic HD gene carriers ($P = .004$ and $P = .01$ for caudate, parametric and nonparametric tests, respectively; and $P = .002$ for the putamen).

Diffusional Study

Values were normally distributed, and there were no outliers. As reported in Table 3 and Fig 2, the MD measured with a planar region-of-interest–based measurement was greater in patients with HD than in controls in both the caudate nucleus ($P < .001$) and the putamen ($P = .002$ and $P = .003$, parametric and nonparametric tests, respectively). In presymptomatic HD gene carriers, the mean diffusivity in the caudate nucleus was lower than that in controls ($P = .04$ and $P = .03$, parametric and nonparametric tests); no differences were found for the putamen.

The intrarater reliability analysis showed strong agreement between the 2 evaluations ($r = 0.98$ for the caudate nucleus and $r = 0.97$ for the putamen; $P < .001$). Similarly, the interrater reliability was 0.98 ($P < .001$) for the diffusivity measurements in both structures.

As reported in Table 3 and Fig 2, the measurements on the segmented volumes yielded results similar to those of planar region-of-interest–based measurements, albeit with differing levels of significance (patients with HD: $P = .001$ and $P = .009$

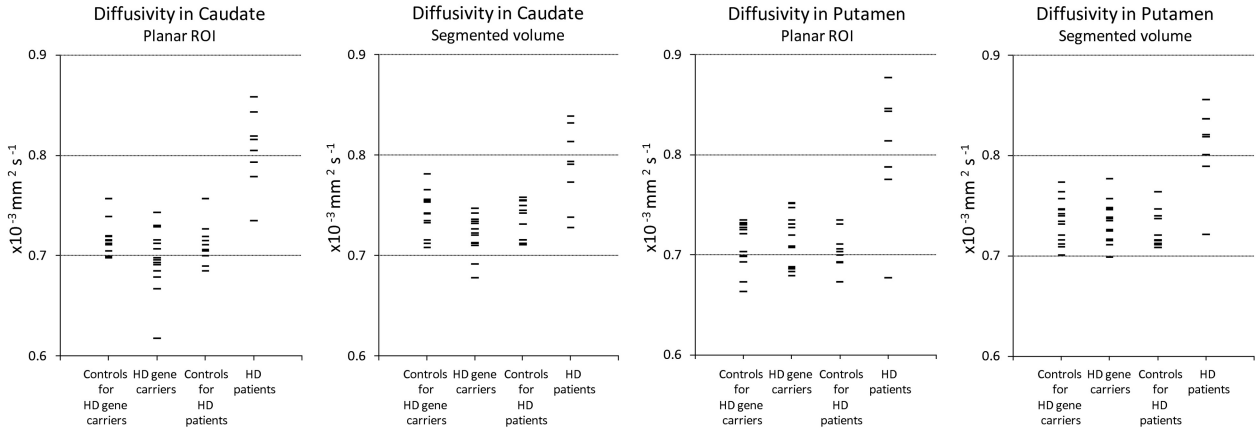

Fig 2. Scatterplots of the diffusivity measurements for the caudate nucleus and putamen.

for the caudate nucleus and $P < .001$ for the putamen; presymptomatic HD gene carriers: $P = .005$ and $P = .006$ for the caudate nucleus).

Discussion

We found that in patients with HD, atrophy of the caudate nucleus and putamen is associated with increased diffusivity, whereas in HD gene carriers far from the predicted onset of their disease, there is decreased diffusivity in the caudate nucleus with a milder neostriatal volume loss.

Reduced volume of the caudate nucleus and putamen in patients with HD is in line with previous studies using both voxel-based morphometry and manual segmentation.[2,3,18,19] Increased diffusivity in these structures has also been previously reported.[7,8] These results are consistent with the known neuropathologic features of HD[20] and with other MR imaging and positron-emission tomography neuroimaging findings, such as decreased *N*-acetylaspartate concentration,[21] glucose metabolism, and dopamine-receptor binding, all pointing to a neurodegenerative process.[22]

Reduced volume of the caudate nucleus and putamen and, in the case of the caudate, also altered diffusivity indicate that structural abnormalities are present in HD gene carriers long before the predicted onset of the clinical symptoms.

A previous study by Rosas et al[9] on presymptomatic HD found increased diffusivity in the putamen but not in the caudate nucleus; the same study, however, did not find altered diffusivity in the caudate nucleus even in symptomatic patients.[9] The cause of the discrepancy remains unclear. It appears possible, however, that it is related to differences in the methods used: While Rosas et al performed voxel-based comparisons, here we considered average diffusivity for the whole segmented caudate and putamen. Voxel-based analysis may reveal topographically limited alterations that are lost when averaging over an extended volume; however, the process of spatial normalization also presents potential sources of error. It has been previously shown that the 2 methods can deliver different results, even on the same dataset.[23]

Recently, increased diffusivity in the caudate nucleus in presymptomatic HD gene carriers has been reported in a conference abstract using voxel-based analysis.[24] The cause for the discrepancy with our findings remains unclear, but it appears plausible that partial voluming effects with the CSF due to atrophy may differently affect voxel-based and volume-based measurements.

The finding of structural alterations long before the onset of symptoms raises the question of whether developmental abnormalities are also present, in addition to the gradual neurodegenerative process. To our knowledge, even neuroimaging studies have not addressed this question; at the time of this writing, 2 neuropathologic studies of presymptomatic HD have found changes in the relative densities of neurons and oligodendrocytes, which were concluded to be more likely related to abnormal development rather than to neurodegeneration.[25,26] Additionally, analysis of longitudinal data on caudate atrophy supports the hypothesis that hypoplasia may be an important determinant of the reduced volume observed in subjects who are still very far from the predicted onset of symptoms.[5]

In contrast with findings in symptomatic patients, our results indicate decreased diffusivity in the caudate nucleus for presymptomatic gene carriers. Decreased diffusivity is not a common finding in neurodegeneration because the gradual rarefaction of barriers due to loss of cell membranes and myelin sheaths typically leads to increased diffusivity.[27] We hypothesize that increased density of oligodendrocytes, demonstrated by pathologic studies, could be a determinant of the observed decreased diffusivity, because oligodendrocytes normally generate myelin sheaths, which are known to be highly restrictive to water diffusion.[25-27] Indeed, it has been shown that in normal subjects the diffusivity in the basal ganglia nuclei follows a pattern inverse to the intensity of myelin staining.[28] The fact that, according to neuropathologic studies, increased oligodendrocyte density is found before the appearance of significant neuronal loss might explain why the MD is initially lower than normal, before increasing as the age of symptom-onset approaches.[25,26] Throughout the course of the disease, putative developmental abnormalities such as increased density of oligodendrocytes and decreased neural density due to incipient neurodegeneration likely compete in determining the observed time course of diffusivity.

The findings of this study, however, do not enable us to exclude other causes of decreased diffusivity. For example, it is well established that iron accumulation results in de-

creased diffusivity measurements due to susceptibility effects.[29] We cannot rule out this as a possible mechanism for the change observed in presymptomatic gene carriers; however, the available neuropathologic studies do not corroborate this hypothesis.[25,26]

The main limitations of the present study are its cross-sectional design and the fact that only 2 groups of patients were considered. Further work, by using a longitudinal design or comparing several groups of patients at different distances from the predicted symptom onset, is needed to confirm our findings that MD is initially reduced in the presymptomatic stage and subsequently increases as neurodegeneration becomes significant. Furthermore, the hypothesis that increased density of oligodendrocytes is the main determinant of the initially decreased diffusivity clearly needs to be confirmed in studies correlating MR imaging and neuropathology.

Conclusions

In line with previous studies, we have found that the neostriatum is already altered in presymptomatic HD gene carriers who are still far from the predicted onset of symptoms. Decreased diffusivity, an atypical finding in neurodegeneration, could be a correlate of increased oligodendroglial population in the caudate nucleus.

References

1. **A novel gene containing a trinucleotide repeat that is expanded and unstable on Huntington's disease chromosomes: Huntington's Disease Collaborative Research Group.** *Cell* 1993;72:971–83
2. Aylward EH, Codori A, Rosenblatt A, et al. **Rate of caudate atrophy in presymptomatic and symptomatic stages of Huntington's disease.** *Mov Disord* 2000; 15:552–60
3. Aylward EH, Rosenblatt A, Field K, et al. **Caudate volume as an outcome measure in clinical trials for Huntington's disease: a pilot study.** *Brain Res Bull* 2003;62:137–41
4. Aylward EH. **Change in MRI striatal volumes as a biomarker in preclinical Huntington's disease.** *Brain Res Bull* 2007;72:152–58. Epub 2006 Nov 2
5. Aylward EH, Sparks BF, Field BA, et al. **Onset and rate of striatal atrophy in preclinical Huntington disease.** *Neurology* 2004;63:66–72
6. Le Bihan D, Turner R, Douek P, et al. **Diffusion MR imaging: clinical applications.** *AJR Am J Roentgenol* 1992;159:591–99
7. Seppi K, Schocke MF, Mair KJ, et al. **Diffusion-weighted imaging in Huntington's disease.** *Mov Disord* 2006;21:1043–47
8. Mascalchi M, Lolli F, Della NR, et al. **Huntington disease: volumetric, diffusion-weighted, and magnetization transfer MR imaging of brain.** *Radiology* 2004;232:867–73
9. Rosas HD, Tuch DS, Hevelone ND, et al. **Diffusion tensor imaging in presymptomatic and early Huntington's disease: selective white matter pathology and its relationship to clinical measures.** *Mov Disord* 2006;21:1317–25
10. **Guidelines for the molecular genetics predictive test in Huntington's disease: International Huntington Association (IHA) and the World Federation of Neurology (WFN) Research Group on Huntington's Chorea.** *Neurology* 1994;44:1533–36
11. Langbehn DR, Brinkman RR, Falush D, et al. **A new model for prediction of the age of onset and penetrance for Huntington's disease based on CAG length.** *Clin Genet* 2004;65:267–77
12. **Unified Huntington's Disease Rating Scale: reliability and consistency—Huntington Study Group.** *Mov Disord* 1996;11:136–42
13. Marder K, Zhao H, Myers RH, et al. **Rate of functional decline in Huntington's disease: Huntington Study Group.** *Neurology* 2000;54:452–58
14. Alemán-Gómez Y, Melie-García L, Valdés-Hernandez P. **IBASPM: toolbox for automatic parcellation of brain structures.** Presented at: 12th Annual Meeting of the Organization for Human Brain Mapping, Florence, Italy, June 11–15, 2006
15. Tzourio-Mazoyer N, Landeau B, Papathanassiou D, et al. **Automated anatomical labeling of activations in SPM using a macroscopic anatomical parcellation of the MNI MRI single-subject brain.** *Neuroimage* 2002;15:273–89
16. Looi JC, Lindberg O, Liberg B, et al. **Volumetrics of the caudate nucleus: reliability and validity of a new manual tracing protocol.** *Psychiatry Res* 2008;163: 279–88
17. Basser PJ, Mattiello J, LeBhian D. **Estimation of the self-diffusion tensor from the NMR spin echo.** *J Magn Reson B* 1994;103:247–54
18. Kassubek J, Juengling FD, Kioschies T, et al. **Topography of cerebral atrophy in early Huntington's disease: a voxel based morphometric MRI study.** *J Neurol Neurosurg Psychiatry* 2004;75:213–20
19. Douaud G, Gaura V, Ribeiro MJ, et al. **Distribution of grey matter atrophy in Huntington's disease patients: a combined ROI-based and voxel-based morphometric study.** *Neuroimage* 2006;32:1562–75
20. Vonsattel JP, Myers RH, Stevens TJ, et al. **Neuropathological classification of Huntington's disease.** *J Neuropathol Exp Neurol* 1985;44:559–77
21. Taylor-Robinson SD, Weeks RA, Bryant DJ, et al. **Proton magnetic resonance spectroscopy in Huntington's disease: evidence in favour of the glutamate excitotoxic theory.** *Mov Disord* 1996;1:167–73
22. Ciarmiello A, Cannella M, Lastoria S, et al. **Brain white-matter volume loss and glucose hypometabolism precede the clinical symptoms of Huntington's disease.** *J Nucl Med* 2006;47:215–22
23. Snook L, Plewes C, Beaulieu C. **Voxel-based versus region of interest analysis in diffusion tensor imaging of neurodevelopment.** *Neuroimage* 2007;34: 243–52
24. Seppi K, Scherfler C, Nocker M, et al. **Diffusion weighted imaging in presymptomatic and early Huntington's disease**. *Mov Dis* 2008;23:77
25. Gomez-Tortosa E, MacDonald ME, Friend JC, et al. **Quantitative neuropathological changes in presymptomatic Huntington's Disease**. *Ann Neurol* 2001; 49:29–34
26. Myers RH, Vonsattel JP, Paskevich PS, et al. **Decreased neuronal and increased oligodendroglial densities in Huntington's disease caudate nucleus.** *J Neuropathol Exp Neurol* 1991;50:729–42
27. Beaulieu C. **The basis of anisotropic water diffusion in the nervous system: a technical review.** *NMR Biomed* 2002;15:435–55
28. Minati L, Aquino D, Rampoldi S, et al. **Biexponential and diffusional kurtosis imaging, and generalised diffusion-tensor imaging (GDTI) with rank-4 tensors: a study in a group of healthy subjects.** *MAGMA* 2007;20:241–53
29. Sener RN. **Echo-planar and gradient-echo diffusion MRI of normal brain iron in the globus pallidus.** *Clin Imaging* 2002;6:371–74